

## Effect of ceria/surfactant molar ratios on the formation of mesoporous ceria nanoparticles and its application in CO<sub>2</sub> capture

Amirul Hafiz Ruhaimi<sup>1</sup>, Haziq Fikri Zaini<sup>1</sup> and Muhammad Arif Ab Aziz<sup>1,2\*</sup>,

<sup>1</sup> School of Chemical and Energy Engineering, Faculty of Engineering, Universiti Teknologi Malaysia (UTM), 81310 UTM Johor Bahru, Johor, Malaysia

<sup>2</sup> Centre of Hydrogen Energy, Institute of Future Energy, Universiti Teknologi Malaysia (UTM), 81310 UTM Johor Bahru, Johor, Malaysia

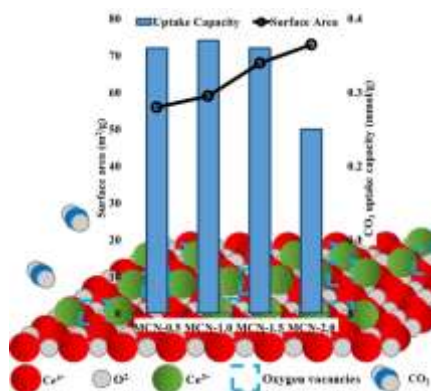
\*Corresponding Author: [m.arif@utm.my](mailto:m.arif@utm.my)

### Article history:

Received 24 August 2020

Accepted 4 November 2020

### GRAPHICAL ABSTRACT



### ABSTRACT

Large quantities of carbon dioxide (CO<sub>2</sub>) in a mixture of natural gas/CO<sub>2</sub> can reduce the heating value of the mixture, reducing the thermal efficiency of a gas engine. Therefore, CO<sub>2</sub> should be separated from the natural gas. CO<sub>2</sub> separation through adsorption method has several advantages, such as high energy efficiency, easy operation, low cost, and availability of different adsorbents. There is a need to develop adsorbents with a porous structure. Several reaction parameters influence the synthesis of porous adsorbents, including temperature, solvent, stirring rates, co-surfactant, pH, and metal to surfactant molar ratio. In this study, the effect of varying ceria to surfactant molar ratio on the synthesis of mesoporous ceria nanoparticles (MCNs) was investigated for CO<sub>2</sub> adsorption. Using cetyltrimethylammonium bromide (CTAB) as a surfactant agent, MCNs were prepared by varying ceria to CTAB molar ratio (0.5, 1.0, 1.5, and 2.0) via a simple hydrothermal method. All the MCN samples showed a bimodal mesoporous structure around 18–30 nm with pore sizes of 3.7 nm. Thermogravimetric analysis showed that the MCNs had weight loss of < 5% when heated up to 1173 K, indicating high thermal stability. MCN-1.0 showed the highest CO<sub>2</sub> adsorption at 0.37 mmol/g, followed by MCN-1.5 and MCN-2.0 at 1 bar and 298 K. We believe that this study will expand the knowledge of ceria material properties towards CO<sub>2</sub> adsorption and will be useful in material selection for industrial CO<sub>2</sub> capture.

**Keywords:** Mesoporous ceria nanoparticle, CO<sub>2</sub> adsorption, hydrothermal

© 2016 © 2020 School of Chemical and Engineering, UTM. All rights reserved  
| eISSN 0128-2581 |

## 1. INTRODUCTION

Natural gas is composed of nitrogen (N<sub>2</sub>), carbon dioxide (CO<sub>2</sub>), methane (CH<sub>4</sub>), and other light hydrocarbons [1]. The heating value of natural gas is the energy released upon combustion under standard conditions, which may be reduced due to the presence of carbon dioxide (CO<sub>2</sub>). Therefore, several industrial sectors employ CO<sub>2</sub> separation systems to improve the quality of natural gas. The three main technologies used to separate CO<sub>2</sub> from natural gas are absorption, membrane separation, and adsorption. The adsorption method has several advantages, such as high energy efficiency, easy operation, lower cost, and availability of different adsorbents [2].

CO<sub>2</sub> can react strongly with oxide surfaces. The oxide surface of cerium oxide (CeO<sub>2</sub>) has been studied extensively. Fourier-transform infrared spectroscopy (FTIR) analysis of CeO<sub>2</sub> at room temperature (25 °C) under the influence of various gases has shown that atmospheric pollutants (e.g.,

water or CO<sub>2</sub>) can be easily adsorbed on CeO<sub>2</sub> surface owing to its high surface reactivity, making the material suitable for CO<sub>2</sub> capture even under ambient conditions [3, 4]. Slostowski et al. studied CO<sub>2</sub> capture using solid CeO<sub>2</sub> nanopowders [4]. Adsorption capacities reached a maximum level of 50 mg of CO<sub>2</sub> adsorbed per gram of CeO<sub>2</sub> for a specific surface area of 200 m<sup>2</sup> g<sup>-1</sup>. In general, high CO<sub>2</sub> capture capacities are dependent on the adsorbent's morphological properties, such as large surface area, and an open and rich nano-porous structure, which provide numerous fully exposed active sites and facilitate rapid gas transportation [5]. In addition, presence of oxygen vacancies attributed to the formation of Ce<sup>3+</sup> in the ceria adsorbent, which provides additional active sites, is considered an important factor for achieving high CO<sub>2</sub> uptake performance [6, 7].

Controlled morphology, including microporous and mesoporous structures, plays a significant role in many adsorption applications [8, 9]. Therefore, it is essential to

fine-tune the specific particle size, surface functionality, and porous structure. The surface properties of metal oxide nanoparticles are influenced by several synthesis parameters, including solvent, temperature, pH, surfactant type, surfactant to material molar ratio, co-surfactant, and stirring rates [10-13]. It is typical for mesoporous materials to employ a template to generate mesoporosity with cationic surfactants, such as cetyltrimethylammonium bromide (CTAB) [10, 14, 15]. Ordered channels are formed within a mesoporous material when the metal oxide self assembles around the template. Azmi et al. studied the sol-gel synthesis of mesoporous ceria nanoparticles (MCNs) using CTAB surfactant [16]. The prepared MCN possessed a high specific surface area ( $76.0 \text{ m}^2 \text{ g}^{-1}$ ), nearly nine-fold more than commercial  $\text{CeO}_2$  ( $8.7 \text{ m}^2 \text{ g}^{-1}$ ). Therefore, it can be deduced that porous structures can be effectively prepared through organic modification using CTAB to enhance the textural properties of the adsorbent. This enhancement is also influenced by the amount of surfactant used. Gao et al. reported that the surface area of the adsorbent increased with an increase in the amount of surfactant used and significantly influenced adsorption uptake performance [10]. Therefore, it is necessary to investigate the effect of the surfactant to material molar ratio on the enhancement of the adsorbent morphology towards  $\text{CO}_2$  adsorption performance.

In this study, MCNs with different ceria to CTAB molar ratios (i.e. 0.5, 1.0, 1.5, and 2.0) were synthesised by a simple hydrothermal method. All the samples were characterised by  $\text{N}_2$  physisorption, FTIR spectroscopy, and thermogravimetric analysis (TGA).  $\text{CO}_2$  adsorption measurements were conducted at ambient temperature and pressure.

## 2. EXPERIMENTAL

### 2.1 Sample Preparation

All the chemicals were of analytical grade (> 98% purity) and purchased from Merck Ltd. The MCNs were prepared via a hydrothermal method. Mixed solutions of CTAB and cerium (III) chloride ( $\text{CeCl}_3$ ) with varying ceria to CTAB surfactant molar ratios (0.5, 1.0, 1.5, and 2.0) were prepared. Aqueous ammonia solution (250 mL of  $\text{NH}_3$ , 25 wt.%) was then added dropwise into a mixed solution with stirring at 293 K until pH 11 was reached. The resulting solution was a gelatinous pale-yellow mixture. Subsequently, the mixture was stirred for another 1 h. Next, the mixture was sealed in a glass vessel and placed in a thermostatic bath at 363 K for 90 h under continuous stirring. It was then cooled to room temperature, and the precipitate was filtered and washed with distilled water. The as-synthesised sample was dried overnight at 333 K followed by calcination at 823 K for 3 h. All samples were designated as MCN-x, where x corresponds to the molar ratio of ceria to the CTAB surfactant.

### 2.2. Characterisation

The Brunauer–Emmett–Teller (BET) analysis of the catalyst was performed by obtaining  $\text{N}_2$  adsorption–desorption isotherms using a Quantachrome Autosorb-1 instrument. The sample was outgassed at 573 K for 3 h before being subjected to  $\text{N}_2$  adsorption. The pore size distributions and pore volumes were determined from the sorption isotherms using the Barrett, Joyner, and Halenda method. An infrared spectrum was recorded on a Cary 600 FTIR spectrometer in the mid-infrared region ( $400\text{--}4000 \text{ cm}^{-1}$ ). The KBr to sample ratio was 100:1 and the sample weight was 35 mg. All the spectra were recorded at room temperature. TGA was conducted in a  $\text{N}_2$  and air mixture from 298 to 1173 K at a heating rate of  $10 \text{ K min}^{-1}$  using a PerkinElmer (STA 8000) thermogravimetric analyser.

### 2.3. $\text{CO}_2$ adsorption performance

The adsorption was tested using a fixed bed U-shaped adsorption column equipped with a  $\text{CO}_2$  analyser (Quantek Instrument Model 906). The pre-treatment step was performed by activating the sample at 413 K for 1 h under flowing  $\text{N}_2$ . Subsequently, a gaseous mixture of 10%  $\text{CO}_2$  and 90%  $\text{N}_2$  at a flow rate of 30 mL/min was introduced into the system at 1 bar and 303 K for 1 h. The desorption step was performed by heating the sample at 413 K for 30 min. The amount of  $\text{CO}_2$  adsorbed was quantified using the area under the curve generated from the adsorption–desorption cycle. A schematic of the experimental  $\text{CO}_2$  adsorption rig is shown in Fig. 1.

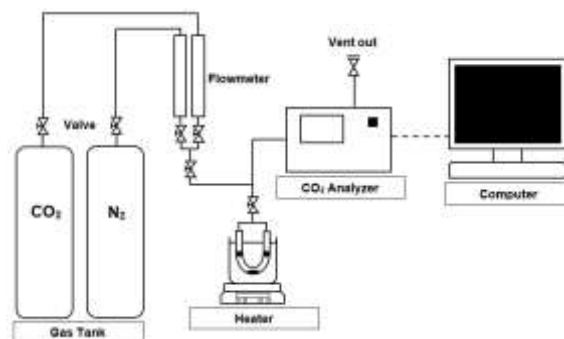


Fig. 1 Schematic of the  $\text{CO}_2$  adsorption test

## 3. RESULTS AND DISCUSSION

Table 1 shows the physical properties of the prepared samples. MCN-2.0 showed the highest BET surface area of  $73 \text{ m}^2/\text{g}$ , followed by MCN-1.5, MCN-1.0, and MCN-0.5. The average pore diameter and pore volume also showed an increasing trend with increasing ceria to surfactant molar ratio (from 0.5 to 2.0). It is well understood that the role of a surfactant is to separate the mixed oxide particles, avoid

sintering, and form small particles that increase the surface area and modify the pore size distribution curves [17-19]. This is supported by a study conducted by Gao et al. [10]. Increasing amount of sodium dodecyl sulphate (SDS) used (0.1–0.5 g) resulted in an increase in the surface area of a magnesium oxide (MgO)-based adsorbent (321.3–501.3 m<sup>2</sup>/g). The prepared MCNs showed higher surface areas than those shown by commercial CeO<sub>2</sub> powder (8.7 m<sup>2</sup>/g) [16].

**Table 1** Physical properties of MCN samples

Sample	BET surface area (m <sup>2</sup> /g)	Average pore diameter (nm)	Pore volume (cm <sup>3</sup> /g)
MCN-0.5	56	7.9	0.111
MCN-1.0	59	7.4	0.110
MCN-1.5	68	8.2	0.139
MCN-2.0	73	8.9	0.162

Fig. 2 shows the nitrogen adsorption–desorption isotherms of all the MCN samples. All isotherms showed a type IV profile, type H1 hysteresis loops (International Union of Pure and Applied Chemistry classification), and characteristics of mesoporous materials with highly uniform cylindrical pores [20]. For all the samples, small hysteresis loops were observed at high partial pressures ( $P/P_0 = 0.9$ ), which was attributed to interparticle textural porosity. The hysteresis loop of the MCN-2.0 sample showed a larger volume compared to the other samples, indicating its larger pore volume, i.e., 0.162 cm<sup>3</sup>/g.

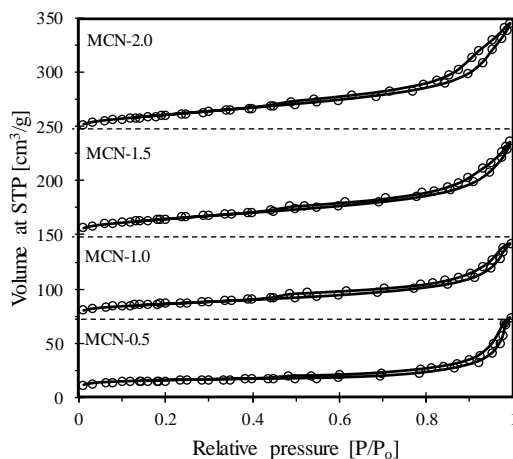


**Fig. 2** Nitrogen adsorption–desorption isotherms of MCN samples

Fig. 3 shows the pore size distributions of all samples. All the samples showed bimodal mesoporous distribution around 18–30 nm with pore sizes of 3.7 nm. A

significant bimodal mesoporous distribution was observed for MCN-2.0 with pore sizes centred at 4 and 18 nm. The high surface area of the MCN adsorbents was mainly attributed to this bimodal mesoporous structure.

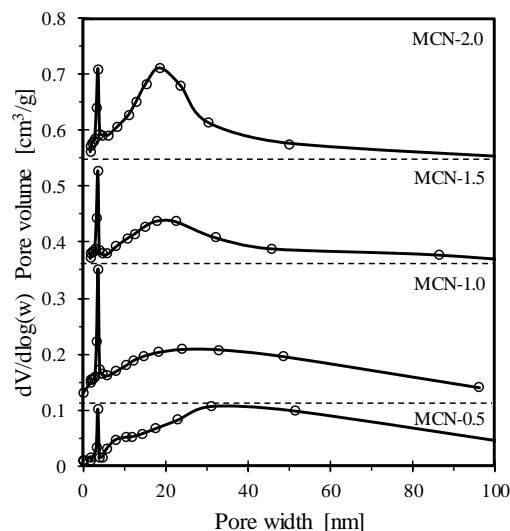


**Fig. 3** Pore size distribution of MCN samples

The FTIR spectra of MCNs with various ceria to surfactant ratios are shown in Fig. 4. The broad band, which appears at 3400 cm<sup>-1</sup>, can be assigned to the O–H stretching vibration of the hydroxyl group on the ceria surface [15]. The band at 2364 cm<sup>-1</sup> arises from the C–H bending vibration of the incorporated surfactant [21]. In addition, the strong band at 1627 cm<sup>-1</sup> can be ascribed to the scissor bending mode of the water molecules [22]. The small peak at 1053 cm<sup>-1</sup> is due to the C–O bond stretching mode, whereas those at 1512, 1417, 719, 602, and 595 cm<sup>-1</sup> may be attributed to the Ce–O stretching vibrations [21, 23].

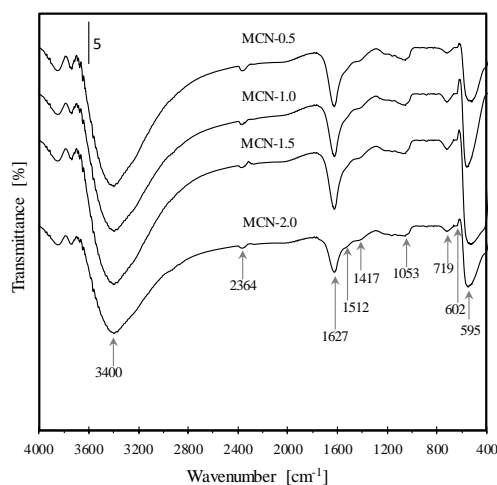


**Fig. 4** FTIR spectrum of MCN samples

To investigate the weight loss of the MCNs with change in temperature, MCN-2.0 was selected (Fig. 5). The studied sample showed an overall weight loss of approximately 4.2% upon heating from 298 to 1173 K. The weight of the sample appeared to decrease rapidly from 373 to 423 K, which could be attributed to the elimination of adsorbed water molecules. Upon a further increase in the temperature, the sample weight appeared to be constant up to 873 K, after which it decreased again, possibly due to decomposition of the CTAB residue remaining from the sample preparation stage.

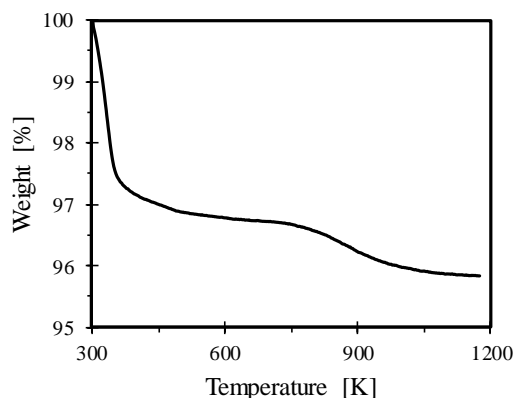


**Fig. 5** TGA analysis of MCN-2.0

Further, this observation indicated that the MCN was prepared without any impurities. As the weight loss was less than 5% when heated to 1173 K, the MCN could be considered to have a high thermal stability.

Fig. 6 shows the adsorption capacities of all the samples. It can be seen that lower metal to surfactant molar ratios resulted in higher CO<sub>2</sub> adsorption. MCN-1.0 showed the highest CO<sub>2</sub> adsorption at 0.37 mmol/g, followed by MCN-1.5 and MCN-2.0. The slightly low uptake capacity exhibited by MCN-0.5 may be because of its low surface area. Although the surface area increased with increasing ceria to CTAB molar ratio (from 1.0 to 2), the number of active surface sites were the highest at the lowest molar ratio. By comparing with other literature reported ceria adsorbent (CeO<sub>2</sub>-P and CeO<sub>2</sub>-SG), MCN 2.0 still considered highest uptake, even-though both adsorbent displayed highest surface area as compared to MCN [16, 24]. This might be contributed by the high contamination of Ce<sup>3+</sup> ions on the CeO<sub>2</sub> which induced the creation of surface oxygen vacancies and increase the adsorbent surface reactivity [25-27]. Oxygen vacancies bind adsorbates (i.e. CO<sub>2</sub>) more strongly than normal oxide sites and role as an additional active site for the adsorbate [7]. This shows that the CO<sub>2</sub> uptake capacity is dependent on the adsorbent surface area, as highlighted by Slostowski et al. [4], and on other factors such as surface reactivity [7, 28]. In addition, the influence

of surfactant over other mesoporous materials such as MgO has been studied by Gao et al. [10]. They found that the MgO surface area, pore size, and pore size distribution depended on the SDS loading. MgO with a high SDS loading (0.1–0.5 g) resulted in better textural properties than with lower SDS loading. However, the CO<sub>2</sub> uptake capacity of MgO loaded with 0.5 g SDS was slightly lower than that with 0.1 g SDS, and it continued to decrease with an increase in the SDS loading.

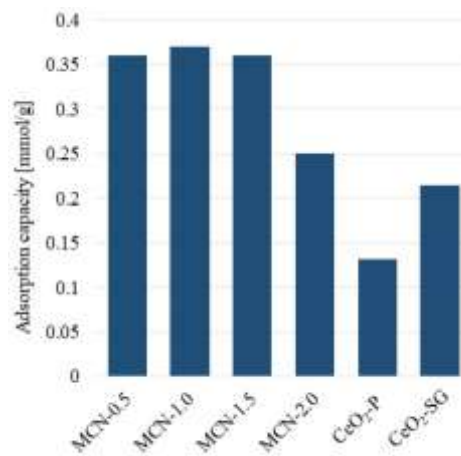


**Fig. 6** CO<sub>2</sub> adsorption capacity of MCN samples and other reported CeO<sub>2</sub> adsorbents under flue gas at ambient atmospheric conditions. CO<sub>2</sub> uptake data of CeO<sub>2</sub>-P (Precipitation method) and CeO<sub>2</sub>-SG (Sol-gel method) adsorbents were obtained from literature [16, 24].

The results of this study are in line with the findings of Kanahara et al., who studied the effect of the preparation method on the CO<sub>2</sub> adsorption performance [28]. They found that besides the surface area, parameters such as crystallite size and surface reactivity also contribute to the adsorption performance. Adsorbent surface reactivity is related to the abundance of oxygen vacancies in the compound, which can provide high adsorption capacity to the final adsorbent [29].

#### 4. CONCLUSIONS

The development of new mesoporous materials for adsorption processes is a promising direction in nanoscience and nanotechnology. By investigating the effects of synthesis parameters, such as the effect of metal on surfactant ratio, it was found that CO<sub>2</sub> adsorption capacity was influenced by the studied parameters. In this study, the effect of varying ceria to CTAB surfactant ratio on the properties of MCN adsorbents towards CO<sub>2</sub> adsorption was investigated. All the MCN samples showed a bimodal mesoporous structure around 18–30 nm with pore sizes of 3.7 nm. Although the surface area increased with increasing

ceria to CTAB molar ratio, the number of active surface sites were the highest at the lowest molar ratio. Therefore, MCN-1.0 showed the highest CO<sub>2</sub> adsorption at 0.370 mmol/g, followed by MCN-1.5 and MCN-2.0. The results obtained in this study advance the knowledge of ceria material properties toward CO<sub>2</sub> adsorption. Further research on the types of surfactants are recommended to improve the adsorbent properties, thus improving the CO<sub>2</sub> adsorption capacity.

## REFERENCES

- [1] M. Kraussler, P. Schindler and H. Hofbauer, *Bioresour Technol.* 237 (2017) 39.
- [2] L. Wang, C. Shi, L. Pan, X. Zhang and J.J. Zou, *Nanoscale.* 12 (2020) 4790.
- [3] C. Li, X. Liu, G. Lu and Y. Wang, *Chinese J. Catal.* 35(8) (2014)1364.
- [4] C. Slostowski, S. Marre, P. Dagault, O. Babot, T. Toupance and C. Aymonier, *J. CO<sub>2</sub> Util.* 20 (2017) 52.
- [5] P. Li, R. Chen, Y. Lin and W. Li, *Chem. Eng. J.* 404 (2021) 126459.
- [6] H. Yu, X. Wang, Z. Shu, M. Fujii and C. Song, *Front. Chem. Sci. Eng.*, 12 (2018) 83.
- [7] C.T. Campbell and C.H.F. Penden, *Science.* 309 (2005) 713.
- [8] A. Alonso, J. Moral-Vico, A.A. Markeb, M. Busquets-Fité, D. Komilis, V. Puentes, A. Sánchez and X. Font, *Sci. Total Environ.* 595 (2017) 51.
- [9] A.A. Azmi and M.A.A Aziz, *J. Environ. Chem. Eng.* 7 (2019) 103022.
- [10] W. Gao, T. Zhou, B. Louis and Q. Wang, *Catalysts.* 7 (2017) 116.
- [11] A.M. Alkadhém, M.A.A. Elgzoly and S.A. Onaizi, *J. Environ. Chem. Eng.* 8 (2020) 103968.
- [12] S. Jin, K.J. Ko and C.H. Lee, *Chem. Eng. J.* 371 (2019) 64.
- [13] M.A.A. Aziz, A.A. Jalil and S. Triwahyono, *Malay. J. Catal.* 3 (2018) 43.
- [14] S. Gnanam and V. Rajendran, *J. Nanopart.* 2013 (2013) 839391.
- [15] A.A. Azmi, A.H. Ruhaimi and M.A.A. Aziz, *Mater. Today Chem.* 16 (2020) 100273.
- [16] A.A. Azmi, N. Ngadi, M.J. Kamaruddin, Z.Y. Zakaria, L.P. Teh, N.H.R. Annuar, H.D. Setiabudi, A.A. Jalil and M.A.A. Aziz, *Chem. Eng. Trans.* 72 (2017) 403.
- [17] A. Maestro, E. Santini, D. Zabiegaj, S. Llamas, F. Ravera, L. Liggieri, F. Ortega, R.G. Rubio and E. Guzman, *Adv. Condens. Matter Phys.* (2015).
- [18] J. Zhang, B. Song, W. Peng, Y. Feng and B. Xu, *Mater. Chem. Phys.* 123(2) (2010) 606.
- [19] X.Y. Yang, L.H. Chen, Y. Li, J.C. Rooke, C. Sanchez and B.L. Su, *Chem. Soc. Rev.* 46(2) (2017) 481.
- [20] M. Thommes, *Chem. Ing. Tech.* 82 (2010) 1059.
- [21] J. Gong, F. Meng, X. Yang, Z. Fan and H. Li, *J. Alloys Compd.* 689 (2016) 606.
- [22] Z.O.R.I.Ț.A. Diaconeasa, L. Barbu-Tudoran, C. Coman, L. Leopold, A. Mesaros, O. Pop, D. RUGINĂ, R. ȘTEFAN, F. TABĂRAN, S. Tripon and C. Socaciu, *Rom. Biotechnol. Lett.* 20 (2015) 10679.
- [23] M.S. Pujar, S.M. Hunagund, V.R. Desai, S. Patil and A.H. Sidarai, *AIP Conf. Proc.* 1942 (2018) 050026.
- [24] K. Yoshikawa, H. Sato, M. Kaneeda and J.N. Kondo, *J. CO<sub>2</sub> Util.* 8 (2014) 34.
- [25] N. Shehata, K. Meehan, M. Hudait and N.Jain, *J. Nanopart. Res.* 14 (2012) 1173.
- [26] E. Shoko, M. Smith and R.H. McKenzie, *J. Phys-Condens. Mat.* 22 (2010) 223201.
- [27] H. Sun, J. Wang, J. Zhao, B. Shen, J. Shi, J. Huang and C. Wu, *Appl. Catal. B.* 244 (2019) 63.
- [28] K. Kanahara and Y. Matsushima, *J. Electrochem.* 166(12) (2019) B978
- [29] A.S. Malik, S.F. Zaman, A.A Al-zahrani, M.A. Daous, H. Driss and L.A. Petrov, *Appl. Catal. A: General.* 560 (2018) 42